EJTP **8, No. 25** (2011) 327–342 *Electronic Journal of Theoretical Physics*

Shell Closures and Structural Information from Nucleon Separation Energies

C. Anu Radha*, V. Ramasubramanian and E. James Jebaseelan Samuel

School of Advanced Sciences, VIT University, Vellore – 632 014, Tamil Nadu. India

Received 27 April 2010, Accepted 16 January 2011, Published 25 May 2011

Abstract: In this work nuclei along N=Z line are of interest as transitions from spherical to deformed shapes are expected to occur when going across the medium mass region. In this respect a strong sudden shape transition between deformation is predicted to occur in the region N=Z as well as N>Z nuclei. New shell gaps are predicted using nucleon and two-nucleon separation energies and the shape evaluation are depicted by applying triaxially deformed cranked Nilsson Strutinsky calculations. Nucleon separation energy plays a major role in the prediction of new magicity in the proton and neutron drip line nuclei.

Keywords: Separation Energy; Stability; Shell Closures; Shape Transition
PACS (2010): 21.10.Gv; 21.10.Dr; 21.10.-k; 21.10.-k; 21.10.Gv

1. Introduction

Nuclear structural calculation far from the region of stability reveals new ideas which are not usually observed in the stability line. These studies provide information about the type of decay and the deformation exhibited by the nuclei. Ground state proton emission is an identification that the drip line has reached. To know about the two proton decay process, their separation energies need to be calculated. The special quality of proton rich nuclei is the diproton emission. Due to pairing, a nucleus with an even number of protons is tightly bound than odd number of proton nucleus [1]. Hence the existence of two proton emission is sensitive to the two proton separation energies. More number of nuclei is found to undergo one proton emission either from the ground state or from an isomeric state or both [2]. When the emitters are found to be deformed, it gives a check for the nuclear structure models at the drip line [3].

Systematic studies related to nucleon separation energies from the masses of nuclei

* canuradha@vit.ac.in

provide evidence for shell closures. It is important to look for new shell closures or the disappearance of existing shell closures from the separation energy calculation [4, 5]. The origin of the unusual stability of nuclei with nucleon numbers 2, 8, 20, 28, 50, 82 and 126, commonly called to as "magic numbers", is explained to be due to nuclear shell structure.At present there is a proliferation of new magic or rather quasi-magic numbers [6, 7]. At the same time some magic numbers are demoted and seem to lose their magicity.

In the simple shell model these are due to shell or sub-shell closures. Shell closure may be demonstrated by a large drop in separation energies. Such phenomena can be simply explained by the simple shell model. The single- and two-nucleon separation energies are fundamental properties of the atomic nucleus [8]. It is a challenge for nuclear many-body theories to derive the shell model out of complex calculations. Systematic of proton and neutron separation energies can be powerful tools to study the nuclear structure at and even beyond the drip lines [9]. It can be used to predict masses and separation energies of nuclei beyond the neutron and proton drip lines.

This paper is organized as follows. Section 1 is introductory. Section 2 deals with the theoretical framework used in the study of shell closures and nuclear structure effects. The found shell gaps, new magicity and shape transitions obtained in the sample case of fp shell region nucleus titanium isotope are discussed in Sec. 3. The evolution of the shapes in the rotating titanium isotopes is also traced in Sec.3. Finally, Sec. 4 contains a summary and conclusion.

2. Theoretical Formalism

An important question in nuclear structure physics is the nature of shape evolution taking place at critical angular momenta near the limit of stability. In order to know the shape of the nucleus before fission, this work involves two formalisms. The first framework shows the nucleon separation energy calculations for various Z and N values in detail. The second formalism depicts the shape transition in the fp shell region nucleus for evolution of shapes in the $\beta-\gamma$ plane at zero temperature using cranked Nilsson Strutinsky calculations with tuned to fixed spins. The shape transitions details are predicted by using potential energy surface calculations.

2.1 Separation Energy for s_p, s_n, s_{2p}, s_{2n} for Different Isotopes and Isotones

Separation energy values for single proton, diproton, single neutron and di neutron are calculated to show the magicity prevailing in their numbers. The separation energies are calculated using the relation

$$S_{2n}(Z,N) = -M(Z,N) + M(Z,N-2) + 2m_n \tag{1}$$

$$S_{2P}(Z,N) = -M(Z,N) + M(Z-2,N) + 2m_P \tag{2}$$

In this work, separation energies are calculated for different proton numbers Z for fixed values of N = 3, 6, 8, 10, 11, 12, 14, 16, 18, 20, 22 and different neutron numbers for various fixed Z values. The mass value for the daughter nuclei are taken from the Audi Wapstra mass table [10]. The same work is extended to two proton separation energy with respect to Z (or N) for fixed neutron (or proton) numbers. Similarly one neutron and two neutron separation energies are calculated for fixed Z and N values.

2.2 Triaxially Deformed Cranked Nilsson Strutinsky Calculation

The second section gives the theoretical framework for obtaining potential energy surfaces of the considered nuclei as a function of deformation β and nonaxiality γ parameters at different spins by the Strutinsky method.

For a non rotating nuclei (zero spin) shell energy calculations assumes a single particle field

$$H_0 = \Sigma\ h_0 \tag{3}$$

where h_0 is the triaxial Nilsson Hamiltonian given by

$$h_0 = \frac{p^2}{2m} + \frac{1}{2}m\sum_{i=1}^{3}\omega_i^2 x_i^2 + Cls + D\left(l^2 - 2\left\langle l^2\right\rangle\right). \tag{4}$$

By Hill-Wheeler parameterization the three oscillator frequencies ω_i are given as include the energy term first

$\mathrm{E}_k = \mathrm{h}\omega_k = \mathrm{h}\omega_{GDR}\ \exp\ [\ -\sqrt{5/4\pi}\ \beta\ \cos\ (\gamma - 2/3\ \mathrm{T}_i\ \mathrm{K})]$

$$\omega_x = \omega_0 \exp\left(-\sqrt{\frac{5}{4\pi}}\ \beta\cos\ \left(\gamma - \frac{2}{3}\pi\right)\right)$$

$$\omega_y = \omega_0 \exp\left(-\sqrt{\frac{5}{4\pi}}\ \beta\cos\ \left(\gamma - \frac{4}{3}\pi\right)\right)$$

and $\omega_z = \omega_0 \exp\left(-\sqrt{\frac{5}{4\pi}}\ \beta\cos\ \gamma\right)$

with the constraint of constant volume for equipotentials

$$\omega_x\omega_y\omega_z = \overset{\circ}{\omega_0^3} = \mathrm{cons\,tan}\,t \tag{5}$$

The values [11] for the Nilsson parameters κ and μ are chosen as

$\kappa = 0.093$ and $\mu = 0.15$

The value for $\hbar\omega_0$ is taken as

$$\hbar\omega_0 \ = \ \frac{45.3\ MeV}{(A^{1/3} + 0.77)} \quad . \tag{6}$$

The same values are used for both protons and neutrons.

The factor 2 in front of $\langle l^2\rangle$ [Eq. (4)] has been used to obtain better agreement between the Strutinsky-smoothed moment of inertia and the rigid rotor value. The parameter D

has been accordingly redetermined with the help of single particle levels in the indicated mass region. Using the matrix elements, the Hamiltonian is diagonalized in cylindrical representation up to N=11 shells.

In a rotating nucleus ($I \neq 0$) without internal excitation, the nucleons move in a cranked Nilsson potential with the deformation described by β and γ. The cranking is performed around the Z-axis and the cranking frequency is ω. Thus, the Hamiltonian for a rotating case is given by

$$H_\omega = H_0 - \omega J_z = \sum h_\omega \tag{7}$$

where

$$h_\omega = h_0 - \omega j_z. \tag{8}$$

Diagonalization of

$$\hbar_\omega \phi_i^\omega = e_i^\omega \phi_i^\omega \tag{9}$$

gives the single particle energy e_i^ω and wave function ϕ_i^ω. The single particle energy in the laboratory system and the spin projections are obtained as

$$\langle e_i \rangle = \langle \phi_i^\omega \left| h_\circ \right| \phi_i^\omega \rangle , \tag{10}$$

and

$$\langle m_i \rangle = \langle \phi_i^\omega \left| j_z \right| \phi_i^\omega \rangle . \tag{11}$$

The shell energy is given by

$$\mathrm{E_{sp}} = \sum \langle \phi_i^\omega \left| h_\circ \right| \phi_i^\omega \rangle = \sum \langle e_i \rangle \tag{12}$$

where

$$\langle e_i \rangle = e_i^\omega + \hbar\omega \langle m_i \rangle . \tag{13}$$

Thus,

$$E_{sp} = \sum e_i^\omega + \hbar\omega I, \tag{14}$$

with the total spin given by

$$\mathrm{I} = \sum \langle m_i \rangle. \tag{15}$$

To overcome the difficulties encountered in the evaluation of total energy for large deformations through the summation of single particle energies, the Strutinsky shell correction method is adapted to $I \neq 0$ cases by suitably tuning [12-14] the angular velocities to yield fixed spins. For unsmoothened single particle level distribution the spin I is given as

$$\mathrm{I} = \int_{-\infty}^{\lambda} g_2 de^\omega = \sum_i \langle m_i \rangle \tag{16}$$

and

$$E_{sp} = \int_{-\infty}^{\lambda} g_1 e^\omega de^\omega + \hbar\omega I = \sum_i e_i^\omega + \hbar\omega I. \tag{17}$$

For the Strutinsky smeared single particle level distribution, Eqs. (16) and (17) transform in to

$$\tilde{I} = \int_{-\infty}^{\lambda} \tilde{g}_2 de^{\omega} = \sum_i \langle \tilde{m}_i \rangle \tag{18}$$

and

$$\tilde{E}_{SP} = \int_{-\infty}^{\lambda} \tilde{g}_1 e^{\omega} de^{\omega} + \hbar\omega \tilde{I} \tag{19}$$

$$= \sum_i^N \tilde{e}_i^{\omega} + \hbar\omega \tilde{I}. \tag{20}$$

In the tuning method the total spin is adapted and is calculated as

$$I = \tilde{I}_z = \sum_{\nu=1}^{N} \left\langle \tilde{J}_z \right\rangle_{\nu}^{\omega} + \sum_{\pi=1}^{\mathrm{Z}} \left\langle \tilde{J}_z \right\rangle_{\pi}^{\omega}. \tag{21}$$

For a chosen integer or half integer spins the above relation permits to select numerically the ω values. The calculations are repeated accordingly as the frequency values $\omega(I)$ change from one deformation point to another.

The total energy is given by

$$E_T = E_{RLDM} + \left(E_{sp} - \tilde{E}_{sp} \right) \tag{22}$$

where

$$E_{RLDM} = E_{LDM} - \frac{1}{2} I_{rig} \omega^2 + \hbar\omega \tilde{I} \quad . \tag{23}$$

The liquid drop energy E_{LDM} is given by the sum of Coulomb and surface energies as

$$E_{LDM}(\beta, \gamma) = [2\chi (B_c - 1) a_s + (B_s - 1)] \tag{24}$$

where B_c and B_s are the relative Coulomb and surface energies of the nucleus. The values used for the parameters a_s and χ are a_s= 19.7 MeV and fissility parameter $\chi = (\mathrm{Z}^2/A)/45$ where Z and A are the charge and mass numbers of the nucleus.

The rigid body moment of inertia I_{rig} is defined by β and γ including the surface diffuseness correction and $\tilde{I}$ is the Strutinsky smoothened spin [15]. For an ellipsoidal shape described by the deformation parameter β and shape parameter γ, the semi axes R_x,R_y, R_z are given by,

$$R_x = R_0 \exp \left[\sqrt{\frac{5}{4\pi}} \beta \cos \left(\gamma - \frac{2\pi}{3} \right) \right]$$

$$R_y = R_0 \exp \left[\sqrt{\frac{5}{4\pi}} \beta \cos \left(\gamma - \frac{4\pi}{3} \right) \right]$$

and $R_z = R_0 \exp \left[\sqrt{\frac{5}{4\pi}} \, \beta \cos \gamma \right]$.

By volume conservation we have

$$R_x R_y R_z = R_0^{03} \tag{25}$$

where R_0^0 is the radius of the spherical nucleus. Here,

$$\mathrm{R_0^0 \ = \ r_0 A^{1/3} \quad (r_0 = 1.16 \ fm) \quad .} \tag{26}$$

The moment of inertia about the Z axis is given by

$$\frac{I_{rig}\left(\beta,\gamma\right)+2Mb^2}{\hbar^2}=\frac{1}{5}\,\frac{AM\left(R_x^2+R_y^2\right)}{\hbar}+\frac{2Mb^2}{\hbar^2} \tag{27}$$

where $2Mb^2$ is the diffuseness correction to the moment of inertia and the diffuseness parameter $b = 0.90$ fm [16,17,18].

The zero temperature potential energy surfaces for fp shell region isotopes have been obtained by the tuned Strutinsky procedure. In the calculation performed here the spin is varied from $I = 0\hbar$ to $30\hbar$ in steps of $2\hbar$, with zero temperature (0.0 MeV), γ from -180 $^\circ$ to -120 $^\circ$ in steps of 10 $^\circ$, and β from 0.0 to 0.8 in steps of 0.1. The Hill Wheeler expressions for the frequencies have been used in the cranked Nilsson model [19]. Since the nuclei considered here ^{44}Ti fall in the region around $28\hbar$, for which calculations have been done for neutron and proton levels separately and shown in the fig.8.

3. Results and Discussions

The fact that all single and two-nucleon separation energies show a similar N/Zdependence suggests an underlying physical reason for this dependence. It is well-known that separation energies of isotopic and isotonic nuclei of a given parity type (even–even, even–odd, odd–even, or odd–odd) follow linear systematic within each shell region if plotted against $N$and Z. The following figures give information about stability and magicity in the light nuclei. Fig.1 and Fig.2 are respectively plots of S_{1p} for fixed N= 3, 6, 8, 10, 11, 12, 14, 16, 18, 20 and 22 plotted as a function of Z and for fixed Z = 3, 6, 8,10, 11, 12, 14, 16, 18, 20 and 22 plotted as a function of N.

Fig.3 and Fig.4 are respectively plots of S_{2p} for fixed N plotted as a function of Z and for fixed Z plotted as a function of N. Neutron separation energies are calculated for fixed isotopes and isotones for varying neutron and proton numbers respectively. Fig. 5 shows the two neutron separation energy variations across the light nuclei and Fig.6 shows the variation of single neutron separation energies with respect to neutron numbers respectively. It is found that new magic numbers appear and some others disappear in moving from stable to exotic nuclei in a rather novel manner due to a particular part of the nucleon-nucleon interaction [20]. We have shown that all single- and two-nucleon separation energies exhibit a similar N/Z behaviour. S_p vs Z shows that $_7N_3$, $_9F_6$, $_{17}Cl_{12}$, $_{21}Sc_{16}$ have $S_p < 0$. Similarly S_p vs.N shows that $_{10}Ne_6$, $_{11}Na_7$ and $_{12}Mg_8$ nuclei are found to have $S_p < 0$. For N=Z the separation energy values are found to be higher. Also for

Z= 8, N=14 is found to be a magic number. For Z=7 to 9, N=16 is found to be a new magic number.

Besides the appearance of new shell closures at Z=6, the conventional shell closures at Z = 20 is on the other hand found to disappear in proton-rich nuclei. A strong kink has been observed in the lower magic numbers across N = 8 and N = 20. This is clearly a measure of shell gaps at the magic numbers. Thus the shell gaps provide a sensitive observable for the shell effects in nuclei. Hence we focus upon S_p and S_{2p} values to explore the nature of shell effects [21].

When adding protons, asymmetry and Coulomb term reduce the binding energy. Therefore steeper drop of proton separation energy is observed and the drip line is reached much sooner. Two-proton separation energies exhibit jumps when crossing magic proton numbers. The magnitude of the jump is a measure of the proton magic shell gap for a given neutron number.

It is shown that separation energies disclose rich nuclear structure information. They indicate very clearly the major shell closures at P = P_{magic} or N=N_{magic} reflected by strong discontinuities of S_p, S_{2p}, S_n and S_{2n} as a function of Z and N. The evolution of nuclear collectivity is reflected as a smooth variation of separation energy as a function of N or Z [4]. First of all, it shows exactly where are the neutron subshell closures and its dependence of the proton number; if the major proton spherical shell closures do not influence the two neutron separation energies, the proton subshell closures due to their nature (proton-neutron interaction) are reflected in the behavior of separation energies. A region of extrastability is found at N=6 for proton numbers Z=3-9. Shell closure is found to be weakened at N=28 in the Z= 15 – 17 region. .

A new shell closure is considered to appear at N=26. A slope change is observed at Z=8 (oxygen isotope). Similar behaviour is observed at Z=18 also. This change in slope confirms the possible change in deformation exhibited by those isotopes during decay clearly shown in fig. 5 having S_{2n} vs N. In the variation of S_n vs N fig. 6 it is found that there is a loss of magicity for nuclei with N=8. N=6 is found to a new magic number for Z=3-9 region.

As a sample case just before fission, the shape of the nucleus can be studied from a titanium isotope. The Fig.7 shows the shape evolution of nucleus from ground state to various spins till the fission limit in the chosen fp shell region nuclei ^{44}Ti which predicts the Jacobi shape transition. Fig.8 gives potential energy surfaces of the considered nuclei as a function of deformation β and nonaxiality γ parameters before fission limit by the Strutinsky method.

Summary and Conclusion

The paper summarizes the main achievements obtained in the field of the single and two nucleon emission studies in last years. Another point which is due to the proton-neutron interaction, the critical point of the transition from spherical to deformed shapes is reflected in the variation of separation energies but the effect is small. The two proton

separation energies and their evolution with neutron and proton number constitute a very good starting point in testing various nuclear structure models. The analysis presented in this paper shows the need of very precise data on masses and extension of this type of information to nuclei very far from stability.

Acknowledgement

The authors thank the VIT University for the support rendered in executing this theoretical calculation.

References

[1] A. Abbas, et al *Multi nucleon forces and the equivalence of different multi cluster structures*, Mod. Phys. Lett. **A16** (2001) 755.

[2] Jorge Rigol, et al *"Shell closure at N=164:spherical or deformed"*, Phys. Rev. **C55(2)**, (1997), 972.

[3] Sakurai, H. et al Phys.Lett.B **448**, (1999) pp 180.

[4] Kanungo, R., et al *"Shell closures in the N & Z = 40-60 region for neutron and proton rich nuclei"*, Phys. Lett. **B649**, (2007) 31.

[5] Samanta, C. et al *"Extension of the Bethe-Weizasacker mass formula to light nuclei and some new shell closures"* Phys.Rev. C **65**, (2002) 037301.

[6] Igal Talmi, et al "*Old and new quasi magic numbers*", From stable beams to exotic nuclei. AIP Conference Proceedings, **1072**, (2008) pp 32.

[7] Sabina Anghel, et al *"Structure features revealed from the two neutron separation energies",* Rom. Journ. Phys., **54**, No.3-4, (2009).301.

[8] Sarazin, F. et al "*Shape Coexistence and the N=28 Shell Closure Far from Stability",* Hyperfine Interactions **132:** 147–152, © 2001 *Kluwer Academic Publishers.*

[9] Lidia S. Ferreira, et al *"Proton emitting nuclei and related topics",* AIP conference proceedings, Portugal, **961**, (2007).

[10] G. Audi, A. H. Wapsta and C.Thibault, "*The Nubase evaluation of nuclear and decay properties"*, Nucl.Phys. **A729** (2003) 337.

[11] Alhassid Y. and Bush B, Nucl. Phys. **A 509**, (1990), 461.

[12] Shanmugam G., Kalpana Sankar and Ramamurthi K, Phys. Rev. C **52**, (1995) 1443.

[13] Shanmugam G., Ramasubramanian V. and Chintalapudi S. N., "*Jacobi shape transition in fp shell nuclei"*, Phys. Rev. C **63**, (2001) 064311.

[14] Shanmugam G. and Selvam V., "*Shape transitions in hot rotating strontium and zirconium isotopes***",** Phys. Rev. C **62**, (2000) 014302.

[15] G. Vijayakumari and V. Ramasubramanian, Int. J. Pure Appl. Sci., (2008) 36.

[16] Maj A. et al, Nucl. Phys. ***A* 687**, (2001a) 192c-197c.

[17] Maj A. et al, Acta Physica Polonica ***B* 32,** (2001b) 2433.

[18] Maj A. et al, Nucl. Phys. ***A* 731**, (2004) 319.

[19] Myers W. D. and Swiatecki W. J., Acta Physica Polonica ***B* 32**, (2001) 1033.

[20] C. Anu Radha, "*Spherical proton emitters"*, M.Phil. Thesis (2005) 97.

[21] C. Anu Radha, E. James Jebaseelan Samuel, "*Magicity from separation energies"*, DAE Int. Symp. on Nucl.Phys. (2009) **54**, 190.

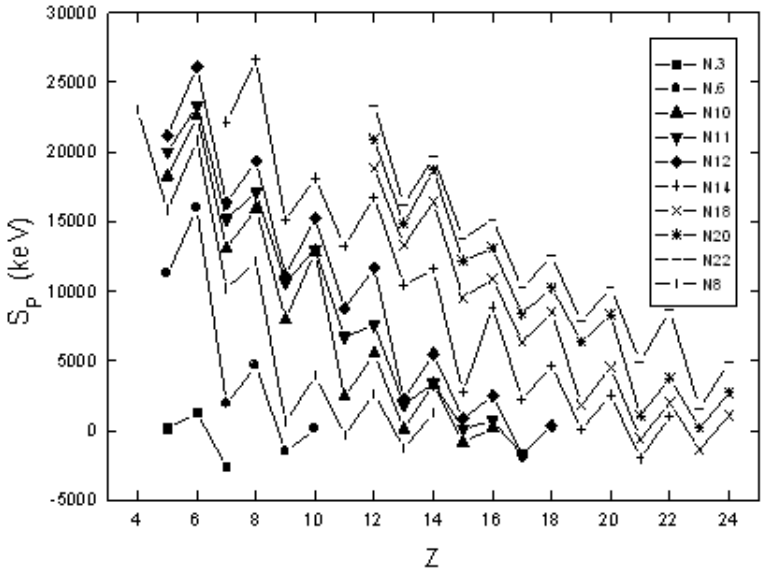

Fig. 1 Separation energy Vs. Z for various N values

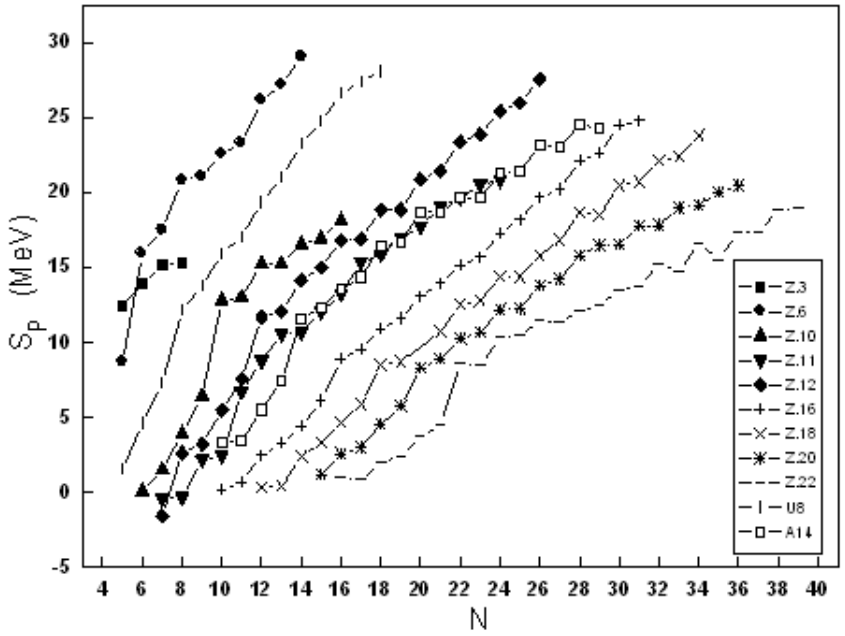

Fig. 2 Separation energy Vs. N for various Z values

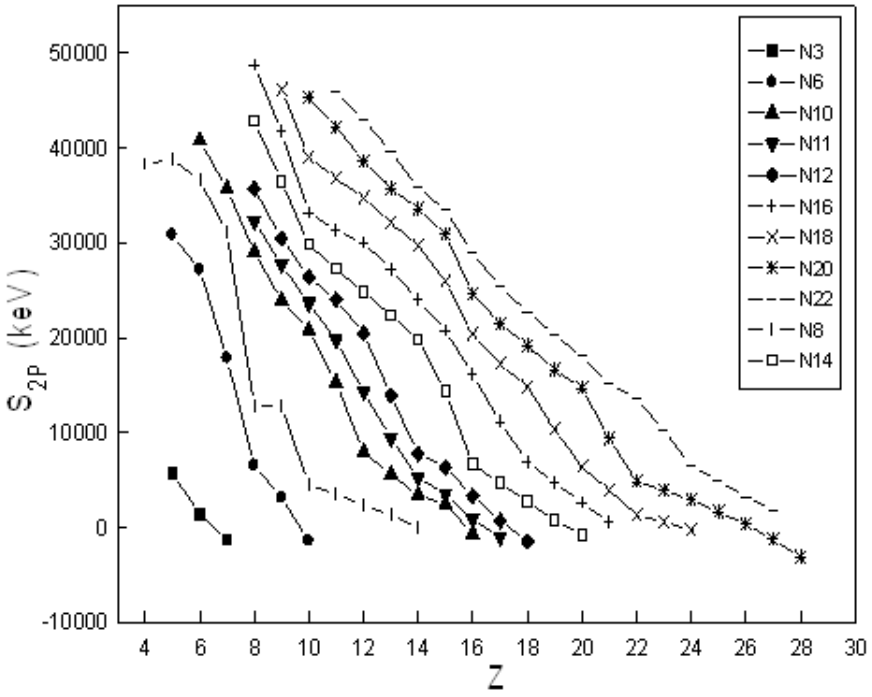

Fig. 3 Two proton separation energy Vs. Z for various N values

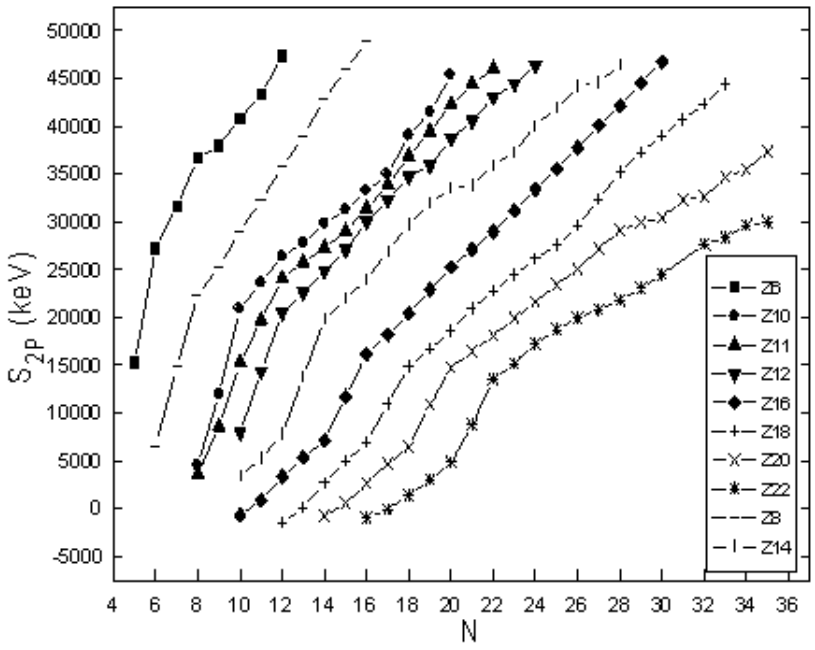

Fig. 4 Two proton separation energy Vs. N for various Z values

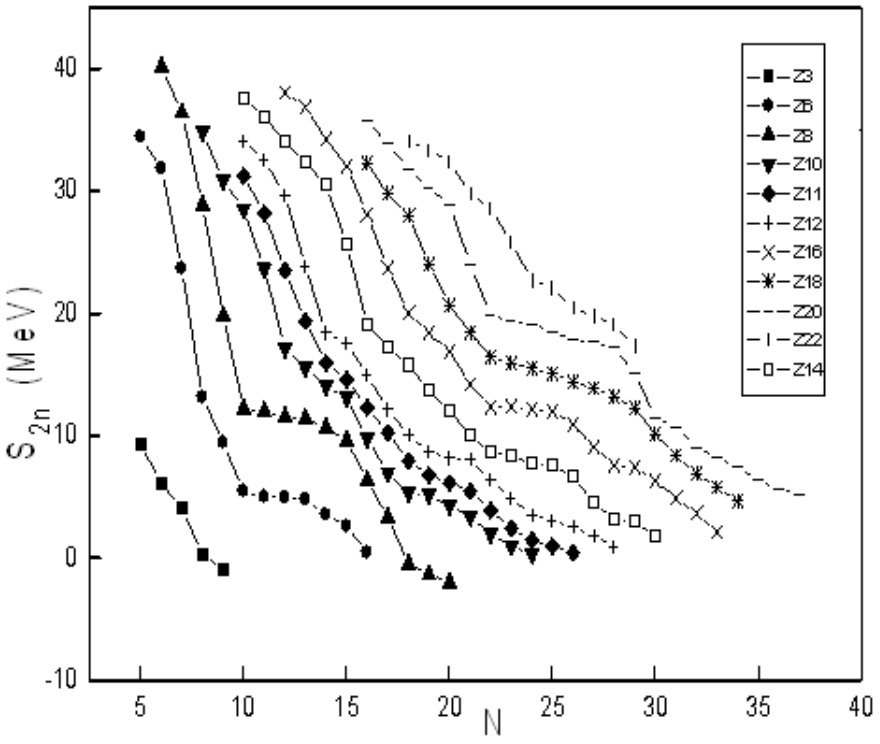

Fig. 5 Two neuton separation energy Vs. N for various Z values

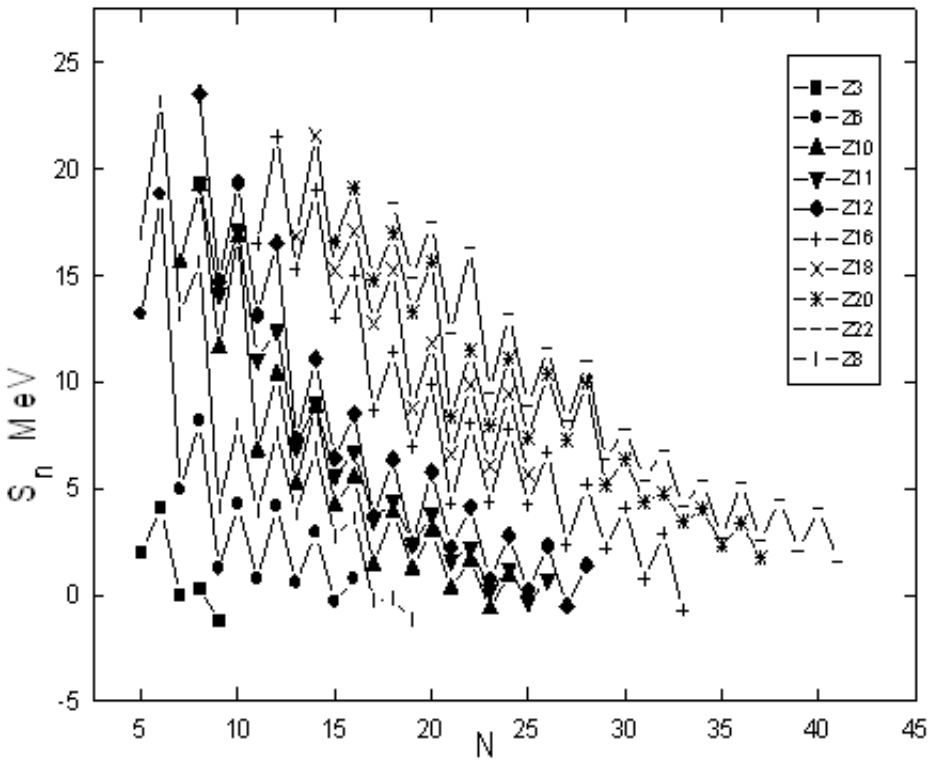

Fig. 6 Single neutron separation energy Vs. N for various Z values

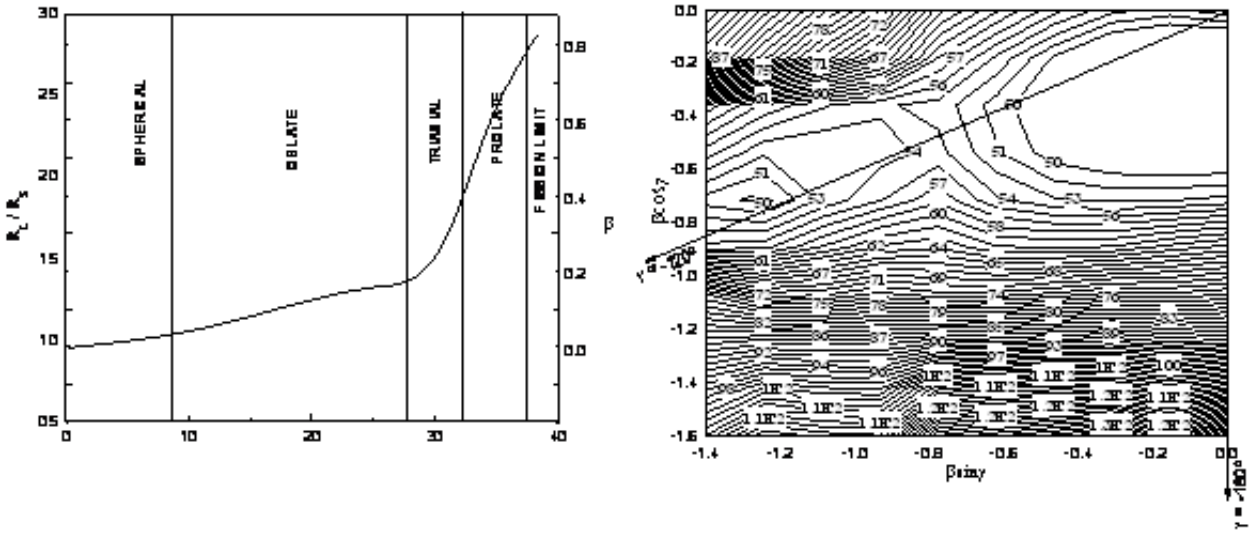

Fig. 7 Shape evolution of ^{44}Ti for various spin values at zero temperature

Fig. 8 Potential energy surface of ^{44}Ti before fission limit at zero temperature